SLAC – PUB – 3611
March 1985
(A)

EFFECTS OF SLOTS/HOLES IN DISKS ON FREQUENCIES OF TM_{01} AND EH_{11} WAVES IN THE DISK-LOADED WAVEGUIDE*

YAO CHONG-GUO

Physics Department, Nanjing University, Nanjing, PRC

and

Stanford Linear Accelerator Center

Stanford University, Stanford, California 94305

ABSTRACT

It has been proven that the combination of boring four holes in each disk at certain radial position R_c and properly reducing the cavity diameter $2b$ can make the frequency of $2\pi/3$ mode for TM_{01} wave invariable and the frequency band for EH_{11} wave rising with respect to the case without holes in disks. Taking the SLAC No. 4 cavity as an example, when $R_c = 28$ mm and hole diameter $2h = 9$ or 11 mm as well as $d(2b) = -0.12$ or -0.28 mm, the operating frequency ($2\pi/3$ mode and TM_{01} wave) maintains still at 2856 MHz but the EH_{11} wave frequency band will move up by about 5.5 or 11 MHz with respect to the case without holes in disks respectively. Obviously, this technique, for example, could be used in Nos. 3, 4 and 5 cavities of the SLAC constant gradient structures for substantially increasing the BBU threshold current of high energy electron linac using SLAC sections as the accelerating tubes.

Submitted to *Nuclear Instruments and Methods*

* Work supported by the Department of Energy, contract DE – AC03 – 76SF00515.

1. Introduction

The increase in the BBU threshold current is very important for the high and medium energy electron linacs because of a larger operating current attainable or a smaller emittance available at certain operating current. For this purpose, many means can be used, among which the improvement in the accelerating structure itself is always fundamental. Despite the constant gradient structure or approximately constant gradient one superior to the constant impedance one in this aspect, many linacs completed and under construction still use several kinds of structure with different dimension variation range [1-4], making further increase in BBU threshold current. SLAC's three-meter long section is unique with truly constant gradient performance. The theoretical analyses and operating experiences at SLAC have indicated that detuning the Nos. 3, 4 and 5 cavities of some sections by 2 or 4 MHz for TM_{01} wave (about 2.5 or 5 MHz for EH_{11} wave as $[(\partial f/\partial b)_{11,\pi}/(\partial f/\partial b)_{01,\,2\pi/3}] = 1.25$ according to our measurements) had considerably raised the BBU threshold current [5-8]. In fact, the first resonance at frequency of about 4139.6 MHz that occurs in the front part of the section with 23.2 cm efficient interaction length between the beam and deflecting wave makes the main contribution to the BBU at pulse width larger than 0.6 μs. The detuning Nos. 3, 4 and 5 cavities of some sections by 2 or 4 MHz obviously means separating the resonations and depressing the couplings of deflecting waves through beam from section to section and is very similar to using three kinds of section with different variation range of dimensions, but much simpler.

The way to do this for SLAC was to squeeze the cavity wall inward. It had three disadvantages. First of all, it is troublesome to do this after the linac has been built. Secondly, after doing this the matching characteristic of the whole section would turn worse, and so it was necessary to readjust the match parameters of the couplers. Figure 1 shows the frequency band performances of the SLAC section with two couplers before and after detuning Nos. 3, 4 and 5 cavities of the section by 4 MHz computed by the method in ref. [9]. Lastly,

the detuning not only created a separation of EH_{11} wave resonations in different sections which is desirable and useful, but also yielded a deviation in phase shift over the cavity from 120° for TM_{01} wave which is hopeless and mischievous. The total phase deviation reaches about 27° over the three cavities when detuning quantity is 4 MHz. Obviously, better the performance and the larger the detuning quantity from the viewpoint of depressing BBU, but this phase deviation may set up a limitation to detuning quantity acceptable. A method of opening four holes symmetrically distributed on disks described below in detail will get the benefits in improvement of BBU threshold current and overcome the three shortcomings mentioned above.

2. The Effects of Slots in Disks on Frequency of TM_{01} Wave

Two slots in each disk shown in fig. 2 bring about a disturbance on cavity fields. The Slater's formula can be used for calculation of the effects if the slot half-width $h \leq t$. The t is the thickness of the disk.

The field strength exponentially decays within the slots, that is

$$H(z) = H(0)\ 10^{-z/2h} \quad .$$

where $H(0)$ is the field strength on the disk surface. Therefore the equivalent depth L of slot should be

$$L = \frac{\int_0^\infty H^2(z)dz}{H^2(0)} = 0.4343h \tag{1}$$

rather than $t/2$. That means the frequency disturbance by holes is in proportion with h^3 instead of h^2. The experiments have verified that this conclusion is correct approximately. The Slater's formula is as follows:

$$\frac{df}{f} = \frac{\frac{1}{2}\int_\tau [E^2 - (Z_0 H)^2]d\tau}{\frac{1}{2}\int_v [E^2 + (Z_0 H)^2]dv} = \frac{D}{S} \tag{2}$$

where τ is the volume disturbed and v the whole cavity volume.

For TM_{01} wave field expressions are:

Within the inside region ($r \leq a$):

$$E_z = \sum_{m=-\infty}^{\infty} A_m \frac{J_0(X_m r)}{J_0(X_m a)} e^{j\beta_m z} \quad ;$$

$$E_r = -j \sum_{m=-\infty}^{\infty} A_m \frac{\beta_m J_1(X_m r)}{X_m J_0(X_m a)} e^{j\beta_m z} \quad ;$$

$$Z_0 H_\theta = j \sum_{m=-\infty}^{\infty} A_m \frac{k J_1(X_m r)}{X_m J_0(X_m a)} e^{j\beta_m z} \quad ;$$

$$E_\theta = H_r = H_z = 0 \quad ;$$

Within the outside region ($a \leq r \leq b$):

$$E_z = \sum_{s=0}^{\infty} a_s \frac{F_0(X_s r)}{F_0(X_s a)} \left\{ \begin{matrix} \cos \\ j \sin \end{matrix} (\eta_s z) \right\} \quad ;$$

$$E_r = -j \sum_{s=0}^{\infty} a_s \frac{\eta_s F_1(X_s r)}{X_s F_0(X_s a)} \left\{ \begin{matrix} j \sin \\ \cos \end{matrix} (\eta_s z) \right\} \quad ;$$

$$Z_0 H_\theta = j \sum_{s=0}^{\infty} a_s \frac{k F_1(X_s r)}{X_s F_0(X_s a)} \left\{ \begin{matrix} \cos \\ j \sin \end{matrix} (\eta_s z) \right\} \quad ;$$

$$E_\theta = H_r = H_z = 0 \quad .$$

Where

$$\beta_m = \beta_0 + \frac{2m\pi}{D} \quad ; \quad X_m^2 = k^2 - \beta_m^2 \quad ;$$

$$\eta_s = \frac{s\pi}{d} \quad ; \quad X_s^2 = k^2 - \eta_s^2 \quad .$$

By matching E_z at $r = a$ the following relation comes:

$$A_m = \frac{1}{D} \sum_{s=0}^{\infty} a_s C_{sm} \quad \text{or} \quad \vec{A} = U \vec{a} \quad . \tag{3}$$

Another relation can be derived from matching H_z at $r = a$:

$$a_s = \frac{X_s}{d}(2-\delta_{s0})\frac{F_0(X_s a)}{F_1(X_s a)}\sum_{m=-\infty}^{\infty} A_m \frac{C_{sm}}{X_m}\frac{J_1(X_m a)}{J_0(X_m a)} \qquad (4)$$

$$\text{or} \quad \vec{a} = V\vec{A}$$

where

$$C_{sm} = \frac{2\beta_m}{\eta_s^2 - \beta_m^2}\begin{cases} (-1)^{(s+2)/2}\sin\frac{\beta_m d}{2} & s \text{ is even,} \\ (-1)^{(s-1)/2}\cos\frac{\beta_m d}{2} & s \text{ is odd.} \end{cases}$$

Combining relation (3) with (4) we find the following homogeneous equation:

$$(UV - I)\,\vec{A} = 0 \quad ; \qquad (5)$$

and from it a dispersion relation follows:

$$|\,UV - I\,| = 0 \quad . \qquad (6)$$

where vectors $\vec{A}(A_0, A_{-1}, A_1, A_{-2}, A_2, \ldots)$ and $\vec{a}(a_0, a_1, a_2, \ldots)$ represent the two sets of field coefficients in two regions, respectively. In solving eq. (5) we can find $\vec{A}$ and then $\vec{a}$ from relation (4).

The electric and magnetic stored energy are equal to each other when resonation occurs. For TM_{01} wave the denominator S of eq. (2) becomes

$$S = \int_v E \cdot E^*\, dv$$

$$= 2\pi D \int_0^a r \sum_{m=-\infty}^{\infty} A_m^2 \left(\frac{\beta_m^2}{X_m^2}\frac{J_1^2(X_m r)}{J_0^2(X_m a)} + \frac{J_0^2(X_m r)}{J_0^2(X_m a)}\right) dr +$$

$$\pi d \int_a^b r \sum_{s=0}^{\infty} a_s^2(1+\delta_{s0})\left(\frac{F_0^2(X_s r)}{F_0^2(X_s a)} + \frac{\eta_s^2}{X_s^2}\frac{F_1^2(X_s r)}{F_0^2(X_s a)}\right) dr$$

Because of $E_r = 0$ on the disk surfaces the numerator D of eq. (2) can be

computed by the formula below in the case of two slots in each disk:

$$D = 0.8686\, h \int_{R_c-h}^{R_c+h} \left\{ F_e \left[\left(\sum_{s=0,2,4,\ldots} a_s \frac{F_0(X_s r)}{F_0(X_s a)} (-1)^{s/2} \right)^2 + \left(\sum_{s=1,3,5,\ldots} a_s \frac{F_0(X_s r)}{F_0(X_s a)} (-1)^{(s-1)/2} \right)^2 \right] - \left[\left(\sum_{s=0,2,4,\ldots} a_s \frac{k}{X_s} \frac{F_1(X_s r)}{F_0(X_s a)} (-1)^{s/2} \right)^2 + \left(\sum_{s=1,3,5,\ldots} a_s \frac{k}{X_s} \frac{F_1(X_s r)}{F_0(X_s a)} (-1)^{(s-1)/2} \right)^2 \right] \right\} \left(d\theta + \frac{2\sqrt{h^2 - (R_c - r)^2}}{r} \right) r dr \quad .$$

Where $F_e = 0.635$ is a factor which comes from electric distribution in slots because of boundary condition $E_t = 0$ on the slot wall.

The effect of four lots on frequency is a factor of two larger than that caused by two slots because of the circular symmetry of field distribution for TM_{01} wave.

3. The Effects of Slots in Disks on Frequency of EH_{11} Wave

The EH_{11} wave is a polarization one. The fields are related to angular coordinate θ. The field expressions are as follows [11]:

Within the inside region $r \leq a$:

$$E_z = \sum_{m=-\infty}^{\infty} A_m \frac{J_1(X_m r)}{J_1(X_m a)} \cos\theta\, e^{j\beta_m z} \quad ;$$

$$E_\theta = -j \sum_{m=-\infty}^{\infty} \left(A_m \frac{\beta_m}{X_m^2 r} \frac{J_1(X_m r)}{J_1(X_m a)} + B_m \frac{k}{X_m} \frac{J_1'(X_m r)}{J_1'(X_m a)} \right) \sin\theta\, e^{j\beta_m z} \quad ;$$

$$E_r = j \sum_{m=-\infty}^{\infty} \left(A_m \frac{\beta_m}{X_m} \frac{J_1'(X_m r)}{J_1(X_m a)} + B_m \frac{k}{X_m^2 r} \frac{J_1(X_m r)}{J_1'(X_m a)} \right) \cos\theta \, e^{j\beta_m z} \quad ;$$

$$Z_0 H_z = \sum_{m=-\infty}^{\infty} B_m \frac{J_1(X_m r)}{J_1'(X_m a)} \sin\theta \, e^{j\beta_m z} \quad ;$$

$$Z_0 H_\theta = j \sum_{m=-\infty}^{\infty} \left(A_m \frac{k}{X_m} \frac{J_1'(X_m r)}{J_1(X_m a)} + B_m \frac{\beta_m}{X_m^2 r} \frac{J_1(X_m r)}{J_1'(X_m a)} \right) \cos\theta \, e^{j\beta_m z} \quad ;$$

$$Z_0 H_r = j \sum_{m=-\infty}^{\infty} \left(A_m \frac{k}{X_m^2 r} \frac{J_1(X_m r)}{J_1(X_m a)} + B_m \frac{\beta_m}{X_m} \frac{J_1'(X_m r)}{J_1'(X_m a)} \right) \sin\theta \, e^{j\beta_m z} \quad .$$

Within the outside region $a \leq r \leq b$:

$$E_z = \sum_{s=0}^{\infty} a_s \frac{F_1(X_s r)}{F_1(X_s a)} \left\{ \begin{matrix} \cos \\ j \sin \end{matrix} (\eta_s z) \right\} \cos\theta \quad ;$$

$$E_\theta = -j \sum_{s=1}^{\infty} \left(a_s \frac{\eta_s}{X_s^2 r} \frac{F_1(X_s r)}{F_1(X_s a)} + b_s \frac{k}{X_s} \frac{f_1'(X_s r)}{f_1'(X_s a)} \right) \left\{ \begin{matrix} j \sin \\ \cos \end{matrix} (\eta_s z) \right\} \sin\theta \quad ;$$

$$E_r = j \sum_{s=1}^{\infty} \left(a_s \frac{\eta_s}{X_s} \frac{F_1'(X_s r)}{F_1(X_s a)} + b_s \frac{k}{X_s^2 r} \frac{f_1(X_s r)}{f_1'(X_s a)} \right) \left\{ \begin{matrix} j \sin \\ \cos \end{matrix} (\eta_s z) \right\} \cos\theta \quad ;$$

$$Z_0 H_z = \sum_{s=1}^{\infty} b_s \frac{f_1(X_s r)}{f_1'(X_s a)} \left\{ \begin{matrix} j \sin \\ \cos \end{matrix} (\eta_s z) \right\} \sin\theta \quad ;$$

$$Z_0 H_\theta = j \sum_{s=0}^{\infty} \left(a_s \frac{k}{X_s} \frac{F_1'(X_s r)}{F_1(X_s a)} + b_s \frac{\eta_s}{X_s^2 r} \frac{f_1(X_s r)}{f_1'(X_s a)} \right) \left\{ \begin{matrix} cos \\ j \sin \end{matrix} (\eta_s z) \right\} \sin\theta \quad ;$$

$$Z_0 H_r = j \sum_{s=0}^{\infty} \left(a_s \frac{k}{X_s^2 r} \frac{F_1(X_s r)}{F_1(X_s a)} + b_s \frac{\eta_s}{X_s} \frac{f_1'(X_s r)}{f_1'(X_s a)} \right) \left\{ \begin{matrix} cos \\ j \sin \end{matrix} (\eta_s z) \right\} \cos\theta \quad .$$

From matching E_z and E_θ at $r = a$ we can find

$$A_m = \frac{1}{D} \sum_{s=0}^{\infty} a_s \, C_{sm}$$

$$B_m = \frac{1}{Dka} \sum_{s=0}^{\infty} a_s \, X_m \left(\frac{\eta_s^2}{X_s^2} - \frac{\beta_m^2}{X_m^2} \right) \frac{C_{sm}}{\beta_m} + \frac{1}{D} \sum_{s=1}^{\infty} b_s \frac{X_m \eta_s}{X_s \beta_m} C_{sm} \qquad (7)$$

$$\text{or } \vec{A} = U \vec{a} \quad .$$

From matching H_z and H_θ at $r = a$ we can find

$$a_s = \frac{X_s}{k}\frac{F_1(X_s a)}{F_1'(X_s a)}\frac{(2-\delta_{s0})}{d}$$
$$\left\{\sum_{m=-\infty}^{\infty} A_m \frac{k}{X_m}\frac{J_1'(X_m a)}{J_1(X_m a)} C_{sm} + \sum_{m=-\infty}^{\infty} B_m \frac{J_1(X_m a)}{J_1'(X_m a)}\left(\frac{\beta_m^2}{X_m^2} - \frac{\eta_s^2}{X_s^2}\right)\frac{C_{sm}}{\beta_m a}\right\}$$

$$b_s = \frac{2\eta_s}{d}\frac{f_1'(X_s a)}{f_1(X_s a)} \sum_{m=-\infty}^{\infty} B_m \frac{J_1(X_m a)}{J_1'(X_m a)}\frac{C_{sm}}{\beta_m}$$

or

$$\vec{a} = V\vec{A} \quad ,$$

where

$$F_1(X_s r) = J_1(X_s r)\, Y_1(X_s b) - Y_1(X_s r)\, J_1(X_s b) \quad ,$$
$$F_1'(X_s r) = J_1'(X_s r)\, Y_1(X_s b) - Y_1'(X_s r)\, J_1(X_s b) \quad ,$$
$$f_1(X_s r) = J_1(X_s r)\, Y_1'(X_s b) - Y_1(X_s r)\, J_1'(X_s b) \quad ,$$
$$f_1'(X_s r) = J_1'(X_s r)\, Y_1'(X_s b) - Y_1'(X_s r)\, J_1'(X_s b) \quad .$$

The equations which are similar to (5) and (6) follow. The vectors $\vec{A}$ (A_0, B_0, A_{-1}, B_{-1}, A_1, B_1, A_{-2}, B_{-2}, A_2, B_2,...) and $\vec{a}$ (a_0, b_1, a_1, b_2, a_2,...) also express the field coefficients within two regions respectively.

When there are two slots in each disk the denominator S of eq. (2) for the EH_{11} wave becomes

$$
\begin{aligned}
S = \pi D \int_0^a \Bigg\{ & \sum_m A_m^2 \frac{J_1^2(X_m r)}{J_1^2(X_m a)} \\
& + \sum_m \left(A_m \frac{\beta_m}{X_m^2 r} \frac{J_1(X_m r)}{J_1(X_m a)} + B_m \frac{k}{X_m} \frac{J_1'(X_m r)}{J_1'(X_m a)} \right)^2 \\
& + \sum_m \left(A_m \frac{\beta_m}{X_m} \frac{J_1'(X_m r)}{J_1(X_m a)} + B_m \frac{k}{X_m^2 r} \frac{J_1(X_m r)}{J_1'(X_m a)} \right)^2 \Bigg\} r\,dr \\
& + \frac{\pi d}{2} \int_a^b \Bigg\{ \sum_s a_s^2 \left(\frac{F_1(X_s r)}{F_1(X_s a)} \right)^2 (1 + \delta_{s0}) \\
& + \sum_s \left(a_s \frac{\eta_s}{X_s^2 r} \frac{F_1(X_s r)}{F_1(X_s a)} + b_s \frac{k}{X_s} \frac{f_1'(X_s r)}{f_1'(X_s a)} \right)^2 \\
& + \sum_s \left(a_s \frac{\eta_s}{X_s} \frac{F_1'(X_s r)}{F_1(X_s a)} + b_s \frac{k}{X_s^2 r} \frac{f_1(X_s r)}{f_1'(X_s a)} \right)^2 \Bigg\} r\,dr \quad .
\end{aligned}
$$

The numerator D of the equation (2) has the following form due to $E_r = E_\theta = H_z = 0$ on the disk surfaces:

$$D = 0.8686\, h\, F_e \int_{R_c-h}^{R_c+h} \int_{\theta_0-\theta(r)/2}^{\theta_0+\theta(r)/2} \cos^2\theta\, d\theta \Bigg\{ \Bigg[\sum_{s=0,2,4,\ldots} a_s \frac{F_1(X_s r)}{F_1(X_s a)} (-1)^{s/2} \Bigg]^2 + \Bigg[\sum_{s=1,3,5,\ldots} a_s \frac{F_1(X_s r)}{F_1(X_s a)} (-1)^{(s-1)/2} \Bigg]^2 \Bigg\} r\, dr$$

$$- 0.8686\, h \Bigg\{ \int_{R_c-h}^{R_c+h} \int_{\theta_0-\theta(r)/2}^{\theta_0+\theta(r)/2} \cos^2\theta\, d\theta$$

$$\Bigg\{ \Bigg[\sum_{s=0,2,4,\ldots} \left(a_s \frac{k}{X_s} \frac{F_1'(X_s r)}{F_1(X_s a)} + b_s \frac{\eta_s}{X_s^2 r} \frac{f_1(X_s r)}{f_1'(X_s a)} \right) (-1)^{s/2} \Bigg]^2$$

$$\Bigg[\sum_{s=1,3,5,\ldots} \left(a_s \frac{k}{X_s} \frac{F_1'(X_s r)}{F_1(X_s a)} + b_s \frac{\eta_s}{X_s^2 r} \frac{f_1(X_s r)}{f_1'(X_s a)} \right) (-1)^{(s-1)/2} \Bigg]^2 \Bigg\} r\, dr$$

$$+ \int_{R_c-h}^{R_c+h} \int_{\theta_0-\theta(r)/2}^{\theta_0+\theta(r)/2} \cos^2\theta\, d\theta$$

$$\Bigg\{ \Bigg[\sum_{s=0,2,4,\ldots} \left(a_s \frac{k}{X_s^2 r} \frac{F_1(X_s r)}{F_1(X_s a)} + b_s \frac{\eta_s}{X_s} \frac{f_1'(X_s r)}{f_1'(X_s a)} \right) (-1)^{s/2} \Bigg]^2$$

$$\Bigg[\sum_{s=1,3,5,\ldots} \left(a_s \frac{k}{X_s^2 r} \frac{F_1(X_s r)}{F_1(X_s a)} + b_s \frac{\eta_s}{X_s} \frac{f_1'(X_s r)}{f_1'(X_s a)} \right) (-1)^{(s-1)/2} \Bigg]^2 \Bigg\} r\, dr \Bigg\}$$

where

$$\frac{\theta(r)}{2} = \frac{d\theta}{2} + \frac{\sqrt{h^2 - (R_c - r)^2}}{r} \quad .$$

$d\theta$ is the angular width of the slots and θ_0 the angular coordinate of the slot center.

Two cases have to be considered as the EH_{11} wave is a polarized one:

(a) $\theta_0 = 0°$: which means the polarization direction is parallel to the line through the centers of two slots.

(b) $\theta_0 = 90°$: which means the polarization direction is perpendicular to the line through the centers of two slots.

The four slots in each disk yield a frequency shift for EH_{11} wave which can be computed by the following simple formula:

$$df \text{ (4 slots)} = df(\theta_0 = 0°, \text{ 2 slots}) + df(\theta_0 = 90°, \text{ 2 slots})$$

In this case there are four polarized waves with polarization directions $\theta_0 = 0°$, $\pm 45°$ and $90°$. Their frequency shifts caused by four slots are all the same and are computed by the above formula.

4. The Results Computed and Measured

The term numbers of the series in the calculations are: $m = 25$ and $s = 13$ for TM_{01} wave; $m = 50$ and $s = 25$ for EH_{11} wave. Obviously, the $2\pi/3$ mode for TM_{01} wave and π mode for EH_{11} wave are most interesting to us. All results given below belong to the case of circular holes ($d\theta = 0°$) for simplicity of machining.

Figure 3 shows the frequency shifts of $2\pi/3$ mode of TM_{01} wave caused by two or four holes in each disk at different radial position R_c. It can be seen that the frequency will move down if holes are placed where the magnetic field is stronger than the electric one. The parameter in the figure is the hole diameter $2h$. The frequency shifts of π mode of EH_{11} wave with $\theta_0 = 0°$ and $90°$ caused by two holes in each disk at different R_c are shown in figs. 4 and 5, respectively.

Figure 6 shows the frequency shifts of π mode of EH_{11} wave caused by four holes in each disk at different R_c with respect to the case without holes in disks on the condition of keeping the frequency of $2\pi/3$ mode of TM_{01} wave invariable that means the corresponding corrections in cavity diameters $2b$ have been made. For example, opening four holes in each disk with $2h = 9$ or 11 mm at $R_c = 28$ mm and reducing the dimension $2b$ by -0.09 or -0.26 mm, the $f(2\pi/3)$ of TM_{01} wave still maintains at 2856 MHz but the frequency bands of EH_{11} wave will

move up by about 4 or 9 MHz respectively. All computations and measurements given above are made with $2\pi/3$ mode cavities of light velocity section of our 20 MeV feed-back electron linac [10]. The dimensions are: $a = 13.90$ mm and $t = 4.00$ mm ($f_0 = 2856$ MHz) and denoted in figure captions. We do the same experiments and calculations with the SLAC No. 4 cavity ($2a = 26.04$ mm and $t = 5.84$ mm) and existence of this effect is again verified. The results are shown in figs. 7 and 8. In this case, when $R_c = 28$ mm, $2h = 9$ or 11 mm with $d(2b) = -0.12$ or -0.28 mm, the frequency bands of EH_{11} wave will rise by about 5.5 or 11 MHz respectively with respect to the case without holes in disks.

The electric coupling through the central holes in disks is dominant in the case of disk-loaded waveguide. Opening holes in disks at $R_c = 28$ mm where the magnetic field is stronger than the electric one will degrade the electric coupling. The measurements show that the decrease in frequency band width is only 2–5%, so that its effect is negligible.

5. Conclusion

This skill is a simple way to build up several kinds of different structures in light of BBU occurrence. The effect of holes in disks on both property of the tube and matching parameters of couplers is negligible if the hole diameter $2h$ is not too big. The skill can be used for SLAC structure to improve linac performance, perhaps it can also be used for other tube design with approximately constant gradient property instead of using several kinds of tube with different dimension variation range to some extent.

In a practical case, of course, the holes should be made without corners and edges to prevent arcing, although all calculations and measurements mentioned above are done with holes of rectangular edge for simplicity.

Acknowledgement

I wish to express my thanks to Professor J. L. Xie of IHEP in China and Dr. G. A. Loew of SLAC in the United States for their kind regards to this work and helpful discussions.

References

1. H. Leboutet, *et al.,* IEEE Trans. Nucl. Sci. **NS-16**, No. 3, 299 (1969).
2. W. Bertozzi, *et al.,* IEEE Trans. Nucl. Sci. **NS-14**, No. 3, 191 (1967).
3. Isamu Sato, Nucl. Instrum. and Meth., **177**, 91 (1980).
4. T. Tomimasu, IEEE Trans. Nucl. Sci. **NS-28**, 3523 (1981).
5. G. A. Loew, *et al.,* Seventh International Conference on High Energy Accelerators, Yerevan, **2**, 229 (1969).
6. F. V. Farinholt, *et al.,* Sixth International Conference on High Energy Accelerators, Cambridge, 90 (1967).
7. R. B. Neal, ed., *The Stanford Two-Mile Accelerator* (W. A. Benjamin, Inc., New York, 1968).
8. R. H. Helm, *et al/.* IEEE Trans. Nucl. Sci. **NS-16**, 311 (1969).
9. V. F. Vikulov, Journal of Technical Physics **52**, 11, 2168 (1982).
10. C. G. Yao, Y. M. Cheng, 20 MeV Feed-back Linac for Therapy, Atomic Energy and Technic (China), **5**, 526 (1979).
11. H. G. Herrward, *et al.,* CERN 63-33.

Figure Captions

fig. 1. The frequency band curves of SLAC structure before (1) and after (2) detuning Nos. 3, 4, and 5 cavities by 4 MHz computed by method in ref. [9].

fig. 2. The denotations of dimensions of slots in disk. The Slots turn to holes if $d\theta = 0°$.

fig. 3. The frequency shifts of $2\pi/3$ mode of TM_{01} wave caused by two or four holes in each disk versus radial position R_c. $2h$ is hole diameter; — computed; - - - measured; cavity dimension: $a = 13.90$ mm; $t = 4.00$ mm.

fig. 4. The frequency shifts of π mode of EH_{11} wave with $\theta_0 = 0°$ caused by two holes in each disk versus radial position R_c. $2h$ is hole diameter; — computed; - - - measured; cavity dimension: $a = 13.90$ mm; $t = 4.00$ mm.

fig. 5. The frequency shifts of π mode of EH_{11} wave with $\theta_0 = 90°$ caused by two holes in each disk versus radial position R_c. $2h$ is hole diameter; — computed; - - - measured; cavity dimension: $a = 13.90$ mm; $t = 4.00$ mm.

fig. 6. The frequency shifts of π mode of EH_{11} wave caused by four holes in each disk versus R_c on condition of $f(2\pi/3) = 2856$ MHz for TM_{01} wave. $2h$ is hole diameter; — computed; - - - measured; cavity dimension: $a = 13.90$ mm; $t = 4.00$ mm.

fig. 7. The frequency shifts of $2\pi/3$ mode of TM_{01} wave caused by two holes in each disk versus radial position R_c. $2h$ is hole diameter; — computed; △ ; ○ ; □ measured; cavity dimension: $2a = 26.04$ mm; $t = 5.84$ mm.

fig. 8. The frequency shifts of π mode of EH_{11} wave caused by four holes in each disk versus R_c on condition of $f(2\pi/3) = 2856$ MHz for TM_{01} wave. $2h$ is hole diameter; — computed; △ ; ○ ; □ measured; cavity dimension: $a = 26.04$ mm; $t = 5.84$ mm.

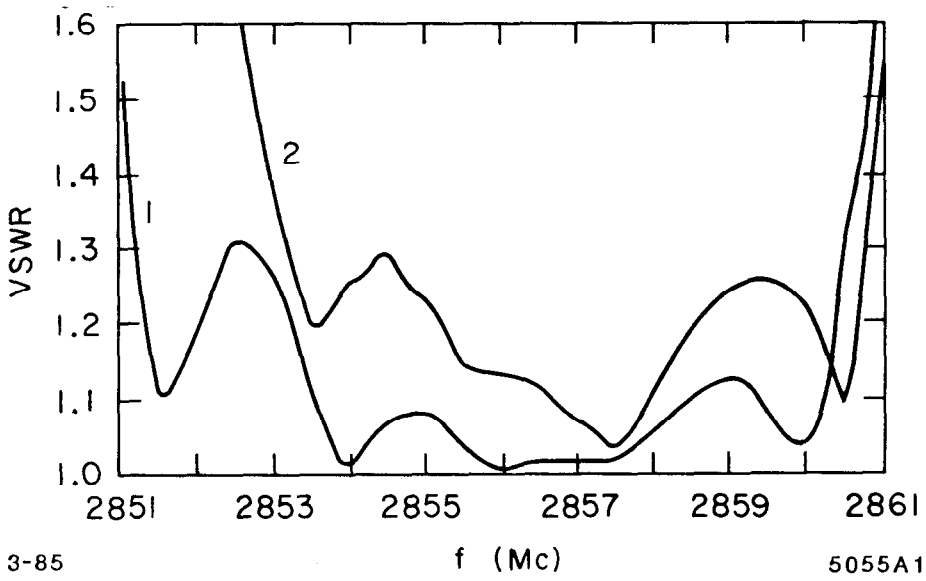
1.6
1.5
1.4
1.3
1.2
1.1
1.0
VSWR
1
2
2851
2853
2855
2857
2859
2861
f (Mc)
3-85
5055A1

Fig. 1

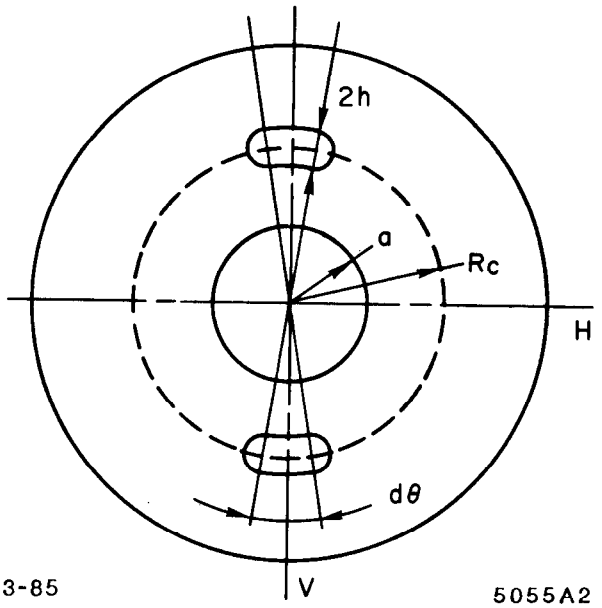

Fig. 2

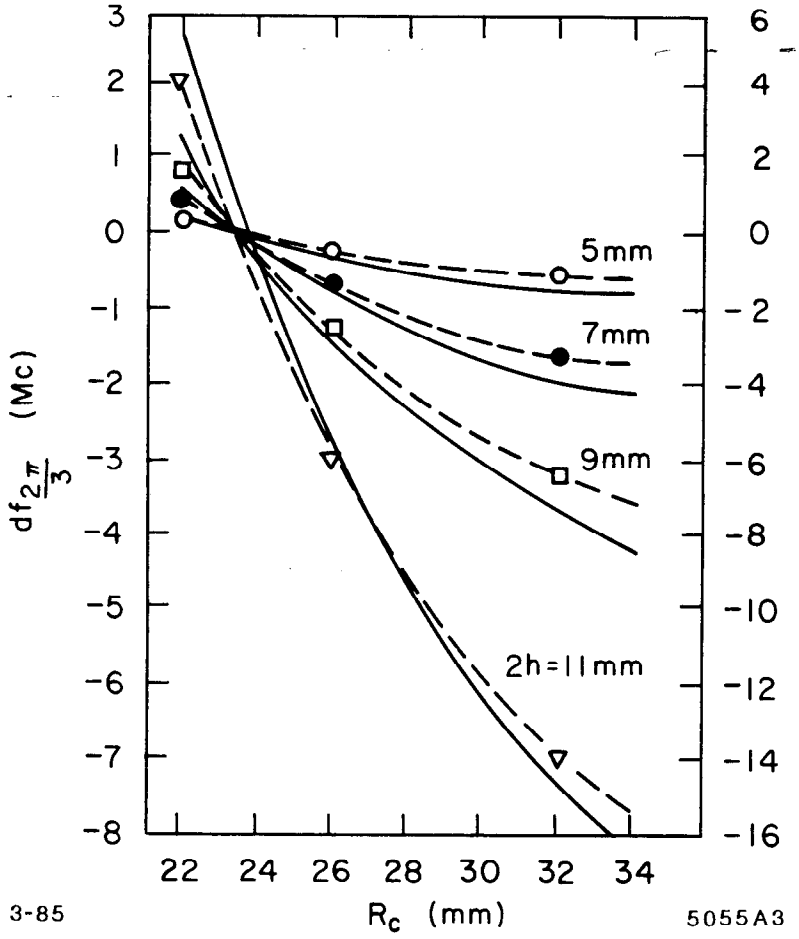
3
2
1
0
-1
-2
-3
-4
-5
-6
-7
-8
6
4
2
0
-2
-4
-6
-8
-10
-12
-14
-16
22
24
26
28
30
32
34
$df_{\frac{2\pi}{3}}$ (Mc)
R_c (mm)
5mm
7mm
9mm
2h=11mm
3-85
5055A3

Fig. 3

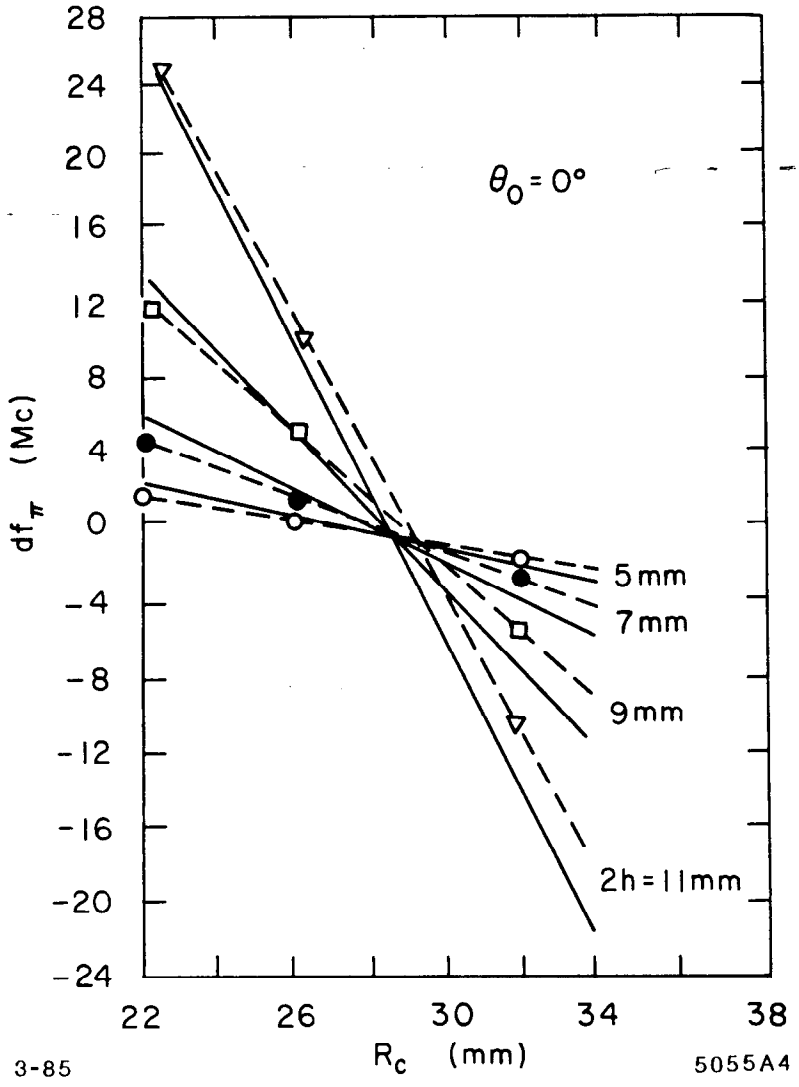
28
24
20
16
12
8
4
0
-4
-8
-12
-16
-20
-24
df_π (Mc)
$\theta_0 = 0°$
5mm
7mm
9mm
2h=11mm
22
26
30
34
38
R_c (mm)
3-85
5055A4

Fig. 4

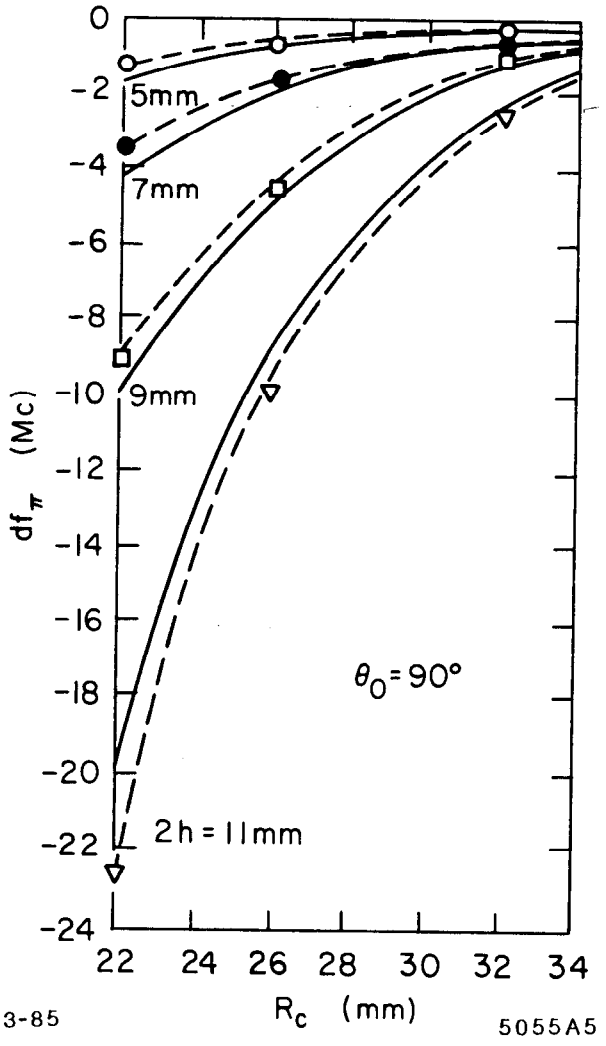
0
-2
-4
-6
-8
-10
-12
-14
-16
-18
-20
-22
-24
5mm
7mm
9mm
2h = 11mm
$\theta_0 = 90°$
df_π (Mc)
22
24
26
28
30
32
34
R_c (mm)
3-85
5055A5

Fig. 5

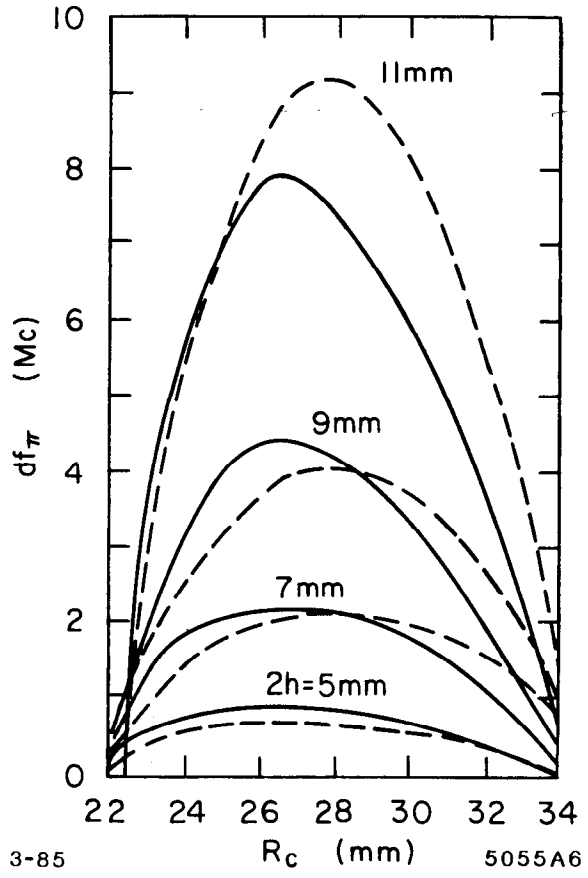
10
8
6
4
2
0
df_π (Mc)
11mm
9mm
7mm
2h=5mm
22
24
26
28
30
32
34
R_c (mm)
3-85
5055A6

Fig. 6

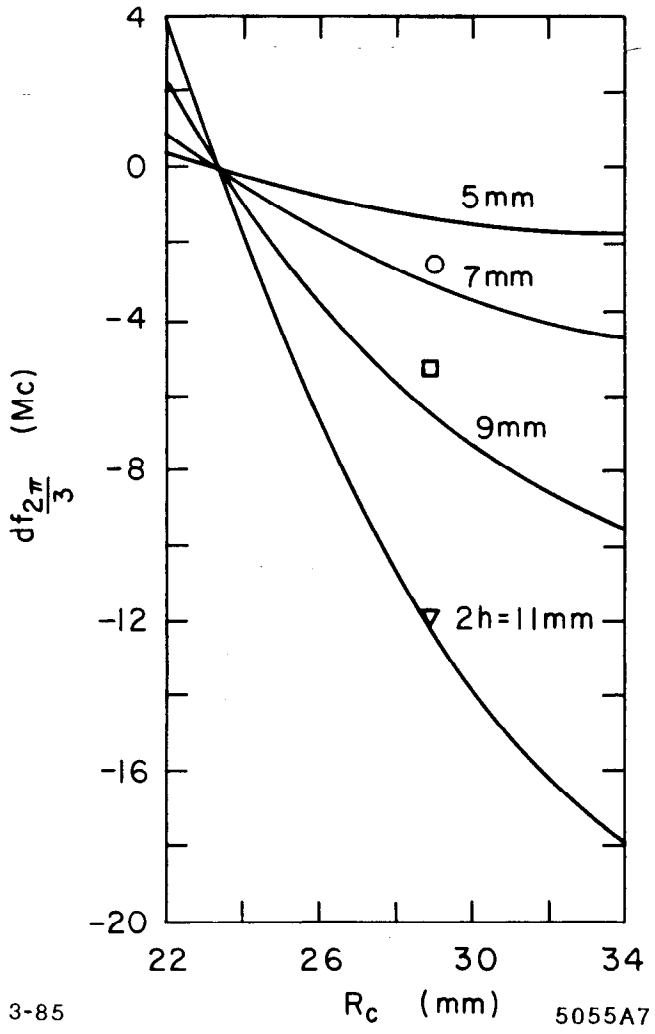
4
0
-4
-8
-12
-16
-20
22
26
30
34
$df_{\frac{2\pi}{3}}$ (Mc)
R_c (mm)
5mm
7mm
9mm
2h=11mm
3-85
5055A7

Fig. 7

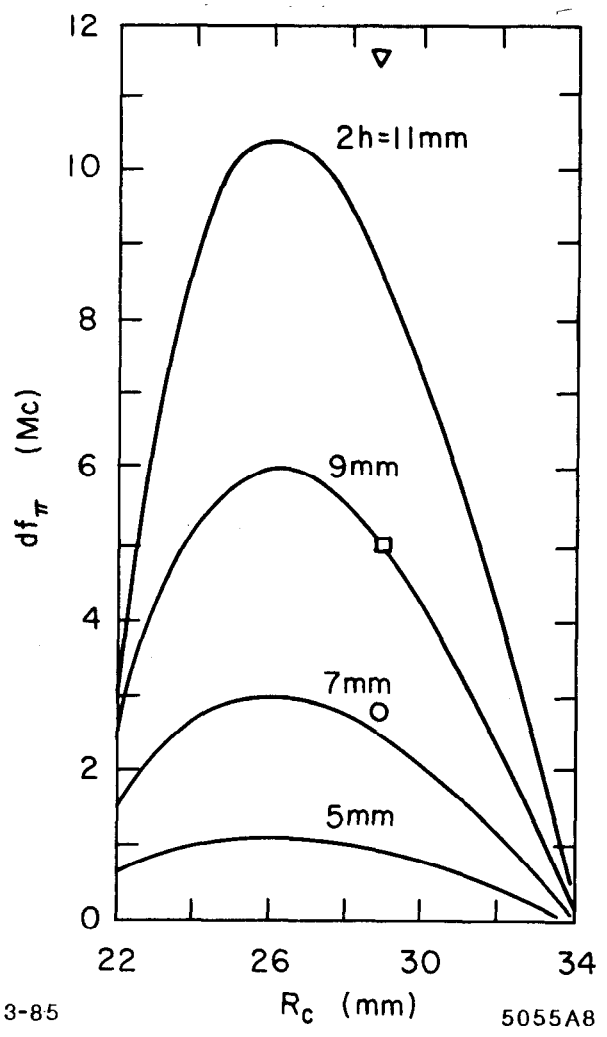
12
10
8
6
4
2
0
df_π (Mc)
2h=11mm
9mm
7mm
5mm
22
26
30
34
R_c (mm)
3-85
5055A8

Fig. 8